An *In Situ* Vapour Phase Hydrothermal Surface Doping Approach for Fabrication of High Performance Co_3O_4 Electrocatalyst with Exceptionally High S-doped Active Surface

Zhijin Tan,[a] Porun Liu,*[a] Haimin Zhang,[a, b] Yun Wang,[a] Mohammad Al-Mamun,[a] Hua Gui Yang,[a] Dan Wang,[a] Zhiyong Tang[a] and Huijun Zhao*[a, b]

[a] *Centre for Clean Environment and Energy, Griffith University, Gold Coast Campus, QLD, 4222, Australia.*

[b] *Key Laboratory of Materials Physics, Centre for Environmental and Energy Nanomaterials, Institute of Solid State Physics, Chinese Academy of Sciences, P.O. Box 1129, Hefei 230031, P.R. China.*

E-mail: h.zhao@griffith.edu.au; p.liu@griffith.edu.au, Fax: +61-7 55528067; Tel: +61-7 55528261

Experimental section

Chemicals and materials

Cobalt (II) nitrate hexahydrate (98%, Sigma-Aldrich), Aluminium sulphide (99%, Sigma-Aldrich), Lithium perchlorate (98%, Sigma-Aldrich), Anhydrous Lithium iodide (99%, Merck), Iodine (99.99%, Sigma-Aldrich), 4-tert-Butylpyridine (TBP, 96%, Acros) and tert-butanol (TBA, 99.5%, Acros), acetonitrile (99%, Sigma-Aldrich) and ethanol (99.5%, Sigma-Aldrich) were purchased and used without further purification. The mesoporous TiO_2 electrodes, Pt electrodes and EL-HPE (I_3^-/I^-) electrolyte were purchased from Dyesol. Deionized water was used throughout the work.

Fabrication of CNS and S-CNS electrodes

The electrodeposition of $Co(OH)_2$ precursor film was performed at room temperature in a three-electrode electrochemical cell, using an FTO substrate as working electrode, a Ag/AgCl electrode as reference electrode and a Pt mesh as counter electrode in an electrolyte containing 0.01 M $Co(NO_3)_2$ and 0.02 M $NaNO_3$ at a constant current of 1.0 mA cm^{-2} for 30s with a CHI 760D Electrochemical Workstation (CH Instruments, Inc.). The obtained $Co(OH)_2$ films were converted to Co_3O_4 counterparts via sintering at 400°C for 30 min in air. The Co_3O_4 nanosheets were readily transformed into S-doped Co_3O_4 nanosheets via an additional H_2S vapour phase hydrothermal (H_2S-VPH) treatment in a closed Teflon-lined

autoclave at 90°C for 6 hours (Fig. S1). Al_2S_3 (0.26 g) and 60 μL water were located at the bottom of the autoclave separately to supply the H_2S dopant source. Lab-made Teflon holder was employed to vertically suspend the Co_3O_4 nanosheet film about 10 cm above the Al_2S_3 and water. After H_2S-VPH treatment, the S-doped Co_3O_4 samples were rinsed in carbon sulphide and ethanol respectively and stored in dark.

DSSCs device fabrication

TiO_2 photoanodes were used after calcination at 500°C for 30 min in air before dye loading (N719, Dyesol, Australia) for 24 h. The dye-loaded TiO_2 electrode was coupled with CEs (CNS, S-CNS, or commercial Pt electrodes) to fabricate the DSSCs; these two electrodes were separated by a 60 μm thick Surlyn and sealed by heating. The electrolyte was injected into the solar cell under vacuum, and the hole was sealed with hot-melt glue.

Characterizations

XRD patterns were collected with a Bruker A8 X-ray diffractometer operated at 40 kV and 30 mA. Room-temperature Raman spectra were measured with a Renishaw 100 system Raman spectrometer (632.8 nm He-Ne laser) with a spectral resolution of 2 cm^{-1} (calibrated using the 520 cm^{-1} silicon band). The X-ray photoelectron spectroscopy (XPS) data was collected with a Kratos Analytical Axis Ultra X–ray photoelectron spectrometer with a Al X-ray source (1.487 keV). C 1s (284.8 eV) was used as the charge reference. The morphological properties of samples were studied by a JSM-7001 field-emission scanning electron microscope (FE-SEM). The microstructures were analyzed by Tecnai 20 (F20) field-emission transmission electron microscope (FE-TEM) with an accelerating voltage of 200kV. For TEM sample preparation, CNS and S-CNS samples were scrapped from FTO substrates, and dispersed in ethanol under ultrasonic. They were transferred onto TEM copper grids by a drop of the solution and drying in air.

Electrochemical measurements

Cyclic voltammetry (CV) measurements were performed with a CHI 760D (CH Instruments, Inc.) electrochemical workstation. FTO supported CNS, S-CNS or Pt electrode, a platinum mash net, and a Ag/AgCl electrode were used as the working electrode, counter electrode, and reference electrode, respectively. A solution of 10.0 mM LiI, 1.0 mM I_2, and 0.1 M $LiClO_4$ in acetonitrile was used as the electrolyte. CV curves were recorded at a scan rate of 50 mV/s. Tafel polarization curves and electrochemical impedance spectra (EIS) were

obtained with symmetrical cells consisting of two identical electrodes; the electrode area was confined to be 0.49 cm^2. The photocurrent-voltage curves were measured using a potentiostat (Model 362, Princeton Applied Research, US). A 500 W Xe lamp (Trusttech Co., Beijing) with an AM 1.5G filter (Sciencetech, Canada) was used as the light source. The light intensity was measured by a radiant power meter (Newport, 70260) coupled with a broadband probe.

Computational Methods

All calculations were performed using the Vienna *ab initio* simulation program (VASP) based on the first-principles density functional theory (DFT) with the projector augmented wave (PAW) method in this study.[1-3] Electron-ion interactions were described using standard PAW potentials,[4, 5] with valence configurations of $3s^2 3p^6 4s^2 3d^7$ for Co, $5s^2 5p^5$ for I, $2s^2 2p^4$ for O, and $3s^2 2p^4$ for S. And a kinetic energy cut-off of 520 eV was set. Herein, we used Perdew-Burke-Ernzerhof (PBE)[6] functional for the GGA-level DFT calculations. Due to the insufficient consideration of the on-site Columbic repulsion, between the Co *d* electrons, DFT may fail to describe the electronic structure of Co_3O_4. To overcome this shortcoming, the GGA+U approach was used.[7] U-J = 6.0 eV for the Co atoms was chosen. A broadening approach proposed by Methfessel and Paxton was employed with an electronic temperature width of 0.2 eV. To simulate the Co_3O_4 (111) surface, a 10-layer slab was enclosed in a supercell with a sufficiently large vacuum region of 15 Å to ensure the periodic images to be well separated. During the geometry optimizations, the atoms in the bottom three layers were fixed at the bulk-like positions; and the rest atoms were allowed to relax until the Hellmann-Feynman forces were smaller than 0.01 eV/Å. Our calculations with the consideration of spin-polarizations demonstrated that the most stable magnetic structures of Co_3O_4 are anti-ferromagnetic. And two neighbouring 4-coodinated Co cations are with opposite spins. To this end, in the middle of our Co_3O_4 (111) surface slab, the two 4-coodinated Co cations are also with the opposite spins in our systems. For Brillouin-zone integrations, gamma-centered *k*-point grids of special points with a (4×4×1) mesh were used for the (1×1) surface cell. The calculation of I adsorption on S-doped Co_3O_4 (111) surface is based on the details described elsewhere.[8]

Figures and captions

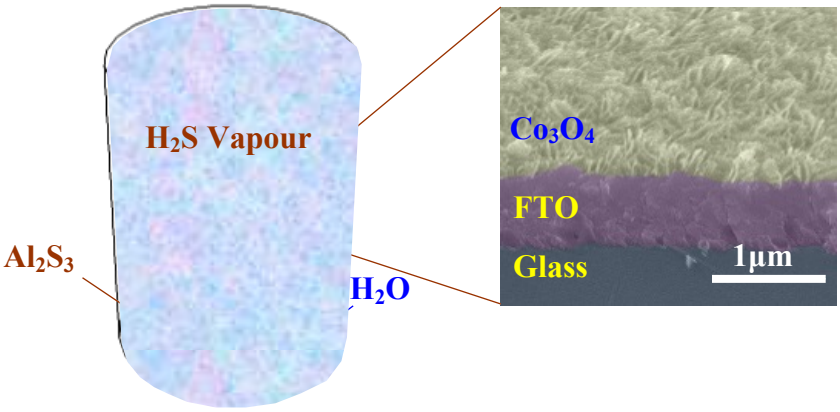

Fig. S1 Schematic illustration of the H_2S-VPH doping setup.

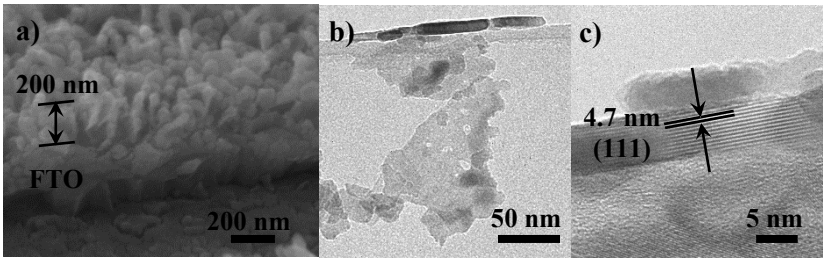

Fig.S2 (a) SEM image, (b) TEM image, and (c) HRTEM image of CNS sample.

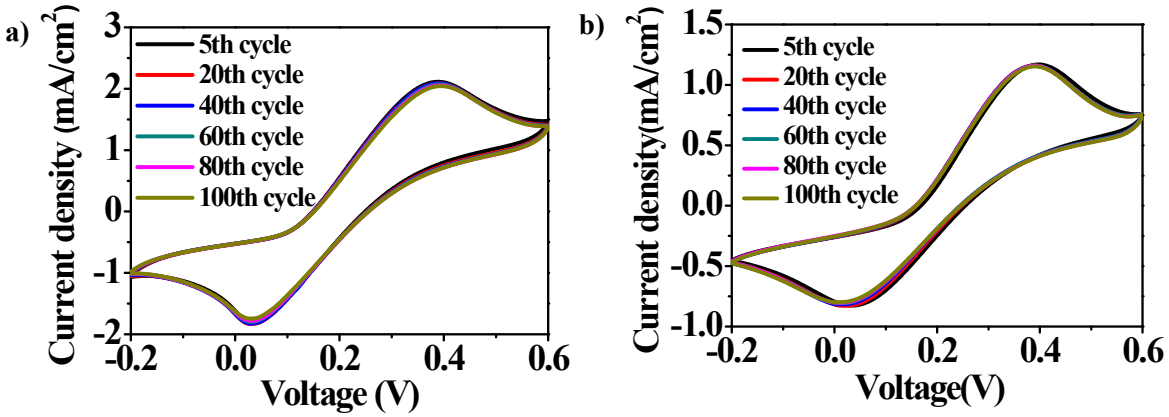

Fig. S3 Consecutive CV curves of a) S-CNS sample and b) Pt in I^-/I_3^- electrolyte.

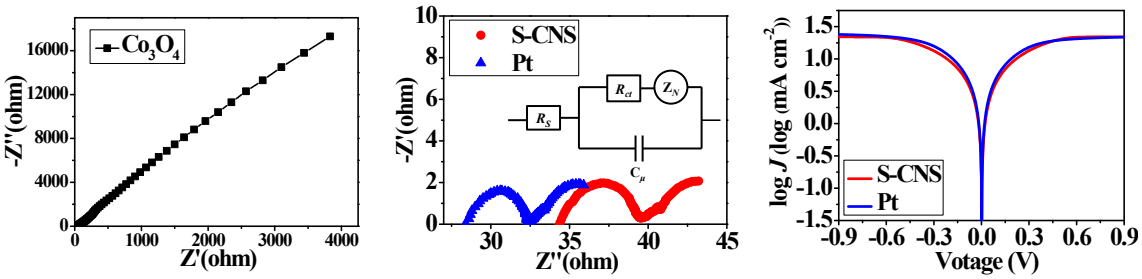

Fig. S4 Nyquist plots of a) CNS, b) S-CNS and Pt electrodes. Inset of b) shows the equivalent circuit. c) Tafel curves of S-CNS and Pt electrodes.

Table.S1 Photovoltaic parameters and EIS parameters of the DSSCs with different electrodes as counter electrode.

Electrode	J_{sc} (mA cm^{-2})	V_{oc} (V)	FF	η (%)	R_s (Ω)	R_{ct} (Ω)
CNS	1.89	0.69	0.25	0.33	-	-
S-CNS	16.83	0.70	0.66	7.79	34.83	4.15
Pt	17.52	0.71	0.66	7.81	28.92	3.13

Electrochemical impedance spectroscopy (EIS) of the symmetrical cells composed of CNS, S-CNS and Pt electrodes was performed to investigate the charge-transfer behaviours and diffusion resistances (Fig. S4a, b). The value of EIS parameters (Table S1) were gained by fitting the EIS data with an equivalent circuit (inset of Fig. S2a). R_s is the series resistance of the electrolyte and electrodes. R_{ct} is the charge-transfer resistance at the electrode-electrolyte interface, which is an indicator for the electrocatalytic activity of the electrode towards the reduction of I_3^-. In strong contrast to the large R_{ct} of CNS electrodes (indicating poor electrocatalytic activity), the similar R_{ct} values of S-CNS and Pt electrodes imply they both possess excellent electrocatalytic activity.

To further examine the electrocatalytic activities, Tafel polarization curve of logarithmic current density as function of potential was collected (Fig. S2b). The exchange current density (J_o), obtained from the extrapolated intercepts of anodic and cathodic branches, is indicative of the electrocatalytic activity. As shown in Fig. S2b, Tafel plot of S-CNS sample exhibits similar slope compared with Pt electrode indicating its good electrocatalytic activity.

Reference

1. G. Kresse and J. Hafner, *Phys. Rev. B*, 1993, **47**, 558-561.
2. G. Kresse and J. Furthmuller, *Comput. Mater. Sci.*, 1996, **6**, 15-50.
3. G. Kresse and D. Joubert, *Phys. Rev. B*, 1999, **59**, 1758-1775.
4. D. Vanderbilt, *Phys. Rev. B*, 1990, **41**, 7892-7895.
5. G. Kresse and J. Hafner, *J. Phys.-Condens. Mat.*, 1994, **6**, 8245-8257.
6. J. P. Perdew, W. Burke and M. Ernzerhof, *Phys. Rev. Lett.*, 1996, **77**, 3865.
7. S. L. Dudarev, G. A. Botton, S. Y. Savrasov, C. J. Humphreys and A. P. Sutton, *Phys. Rev. B*, 1998, **57**, 1505-1509.
8. Y. Hou, D. Wang, X. H. Yang, W. Q. Fang, B. Zhang, H. F. Wang, G. Z. Lu, P. Hu, H. J. Zhao and H. G. Yang, *Nat. Commun.*, 2013, **4**, 1583